Earth Surface Processes and Landforms
Earth Surf. Process. Landforms **23**, 927–941 (1998)

ENERGETICS PREDICTION OF FREQUENCY-DEPENDENT SUSPENDED SAND TRANSPORT RATES ON A MACROTIDAL BEACH

YOLANDA FOOTE[1]*, PAUL RUSSELL[1], DAVID HUNTLEY[1] AND PETER SIMS[2]
[1] *Institute of Marine Studies, University of Plymouth, Drake Circus, Plymouth, PL4 8AA, UK*
[2] *Department of Geographical Sciences, University of Plymouth, Drake Circus, Plymouth, UK*

Received 19 February 1997; Revised 9 March 1998; Accepted 1 May 1998

ABSTRACT

The on–offshore (cross-shore) transport of sand on beaches is highly time-variable, which has made it difficult to model or predict. In this paper, simple energetics modelling is used to compare velocity moment predictions with field observations of suspended sand transport rates. Separate consideration is given to transport associated with the three main frequency-dependent cross-shore transport processes: that associated with the short (incident) waves, that due to the long (infragravity) waves, and transport associated with the mean flow.

Direct comparison between the depth-averaged model predictions, and the in-situ point measurements was facilitated by making the first order assumption that the time-averaged suspension profile is exponential and the wave velocity profile is vertically uniform. An appropriate rippled bed roughness was used to provide the drag coefficient in the energetics model and the vertical length scale of the exponential suspension profile.

Despite these simple assumptions, comparison of the velocity moment predictions with the field observations of suspended sand fluxes reveals that this approach has the capacity to predict transport magnitudes due to short wave, long wave, and mean flow components to within about one order of magnitude. However, owing to the limitations of the model, the transport direction of the short wave component could not, on occasion, be correctly determined, probably due to 'reverse' transport over ripples. © 1998 John Wiley & Sons, Ltd.

KEY WORDS: beach sediments; cross-shore sand transport; fluid energetics modelling; velocity moments; suspended sand fluxes; wave frequency components; predictions of sand transport fluxes

INTRODUCTION

Bagnold (1956, 1963, 1966) developed a sediment transport model for uni-directional fluvial environments using a fluid energetics approach, whereby the local sediment transport rate was related to the cube ('energy') of the instantaneous velocity. These energetics formulations have been incorporated into several studies of cross-shore transport processes, (e.g. Bowen, 1980; Bailard and Inman, 1981; Guza and Thornton, 1985; Roelvink and Stive, 1989; Roelvink, 1993; Kroon, 1994). Guza and Thornton (1985), for example, applied field data to the sediment transport model by Bailard (1981) in order to determine the dominant terms in the bedload and suspended load transport modes.

In this paper, division of the dominant suspended load transport term into different frequency component subterms is used to demonstrate the relative importance of the long period, short period and mean flow contributions of the flow field (Foote, 1994; Foote and Huntley, 1994; Foote *et al*., 1994). Comparison of the suspended load velocity moment predictions with field measurements is then used to assess the validity of this energetics approach in the prediction of cross-shore suspended sand transport fluxes.

FIELD MEASUREMENTS

Field Site

A field experiment was carried out at Spurn Head, Yorkshire, on the northeast coast of England during April 1991 by the British Beach and Nearshore Dynamics (B-BAND) project (Russell *et al*., 1991; Davidson *et al*.,

* Correspondence to: Dr Y. Foote, c/o Institute of Marine Studies, University of Plymouth, Drake Circus, Plymouth, PL4 8AA.
Contract/grant sponsor: Natural Environment Research Council; contract/grant number: GR9/1484

CCC 0197-9337/98/100927–15 $17.50

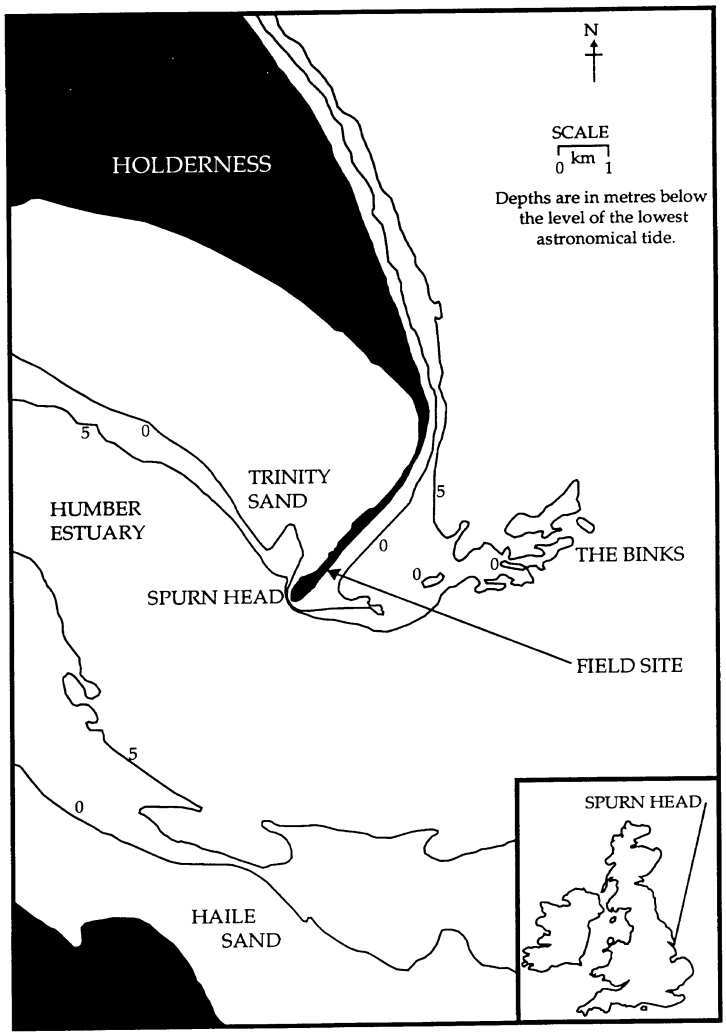

Figure 1. Location of B-BAND Fieldwork Site at Spurn Head (April, 1991).

1993a). Spurn Head is a hook-shaped spit of sand and shingle attached to the southern end of the Holderness coastline, extending 5·6 km in length, of variable width and subject to breaching. The Holderness coast comprises a thin sand and shingle beach overlying a wave-cut platform of glacial deposits, backed by a rapidly disappearing glacial till cliff with erosion rates of the order of $2\,m\,a^{-1}$ (e.g. Pringle, 1985; Mason and Hansom, 1988; Hoad, 1991).

The B-BAND field site was located on the seaward side of the sand spit facing the North Sea (Figure 1). The beach is exposed to wind-driven waves from the North Sea, and also to episodic swell waves which originate in the Norwegian Sea and approach mainly from the northeast. The tidal range varies between 7 m on spring tides and 3 m on neap tides. Figure 2 shows beach profiles for the B-BAND field site on two days, 18 and 23 April 1991, with average gradients from 0·0975 over the high tide beach face, to 0·023 on the low tide terrace. The profile comprised a lens of fine to medium gravel over the high tide upper beach face with well sorted medium sands ($D_{50} = 0{\cdot}35$ mm) at the sensor array location on the low tide terrace. According to the morphodynamic classification system of Short (1991), the beach is intermediate. The breaking wave types are predominantly plunging on the high tide beach face and more spilling on the low tide terrace.

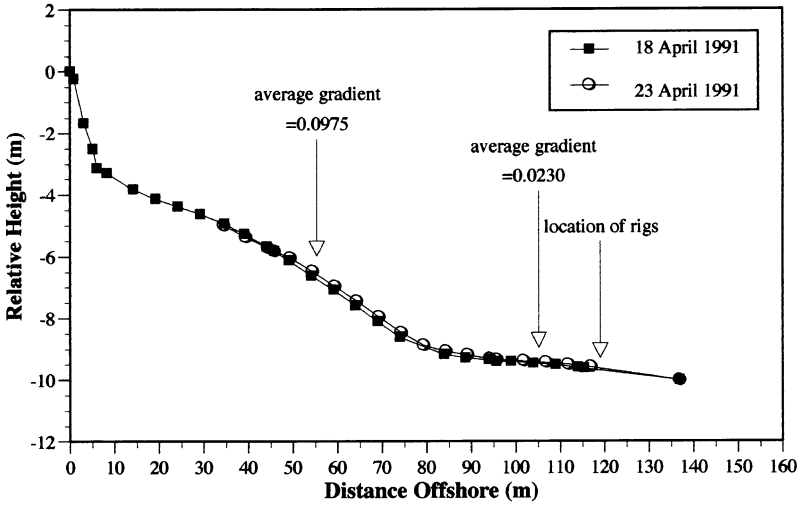

Figure 2. Beach Profile at Spurn Head on 18 and 23 April, 1991 (average gradient values and location of the sensor rigs are shown).

Data collection

Instrumentation used in the Spurn Head experiment comprised pressure transducers (PTs), a range of electromagnetic current meters (EMCMs), and optical backscatter sensors (OBSs). Four instrument rigs were deployed at the corners of a 20 m by 20 m square array, on the lower foreshore of the beach. An instrument rig typically consisted of three EMCMs (0·10, 0·25 and 0·63 m above the bed), three OBSs (0·04, 0·10 and 0·63 m above the bed) and one PT. At the start of the fieldwork (16 April) conditions were dominated by a violent storm event, with breaking wave heights, $H_b \approx 3$ m, which towards the end of the field deployment period (23 April), gave way to calmer weather and regular 'groupy' waves ($H_b \approx 1$ m). This study focuses on measurements collected at one instrument station during two days (18 and 23 April 1991). A more detailed description of the fieldwork and techniques used can be found in Russell *et al*. (1991) and Davidson *et al*. (1993a).

CROSS-SHORE SUSPENDED SAND TRANSPORT

Suspended sediment concentration and cross-shore current velocity data are examined, using an energetics-based approach, with the primary aim of predicting the cross-shore fluxes of sand which arise through the interaction of mean flows, short waves and long waves.

Suspended sand transport rate predictors

The cross-shore transport model developed by Bailard (1981, 1982, 1987) was based on Bagnold's (1956, 1963, 1966) total load sediment transport model for uni-directional stream conditions, and provides an estimate of the cross-shore and longshore transport rates in both the bed and suspended loads. Bailard (1981) suggested that the time-averaged cross-shore immersed weight sand transport rate, $\langle i_x \rangle$, could be modelled as:

$$\langle i_x \rangle = \rho C_f U_m^3 \left\{ \begin{array}{l} \dfrac{\varepsilon_B}{\tan\phi}\left[\dfrac{\langle |u|^2 u\rangle}{U_m^3} - \dfrac{\tan\beta}{\tan\phi} U3^*\right] \\ +\varepsilon_S \dfrac{U_m}{W}\left[\dfrac{\langle |u|^3 u\rangle}{U_m^4} - \varepsilon_S \dfrac{U_m}{W}\tan\beta\, U5^*\right] \end{array} \right\} \quad (1)$$

where ρ is the density of sea water, C_f is the coefficient for drag at the sea bed, U_m is the maximum orbital velocity (defined below), ε_B and ε_S are the bed and suspended load efficiencies, respectively, $U3^*$ and $U5^*$

(defined below in Equations 3 and 4) are even cross-shore velocity moments, W is the fall velocity of the sediment, $\tan\beta$ is the local beach slope and $\tan\phi$ is the angle of repose. For the Spurn Head dataset, the fixed coefficients have been given the following values: $\rho = 1025\,\mathrm{kg\,m^{-3}}$; $W = 0{\cdot}047\,\mathrm{m\,s^{-1}}$; $\tan\beta = 0{\cdot}023$; $\tan\phi = 0{\cdot}65$. The remaining parameters are defined as follows:

$$U_m = 2^{1/2}\langle \tilde{u}^2 \rangle^{1/2} \quad \text{the maximum orbital velocity} \tag{2}$$

$$(U3^*) = \langle |u|^3 \rangle / U_m{}^3 \quad \text{the third central even moment} \tag{3}$$

$$(U5^*) = \langle |u|^5 \rangle / U_m{}^5 \quad \text{the fifth central even moment} \tag{4}$$

where, $|u|$ represents the modulus of the velocity, $\bar{u}$ the mean velocity component, $\tilde{u}$ the fluctuating velocity component and angle brackets denote time-averaged quantities.

The basic assumptions underlying this energetics approach to sediment transport can be summarized as follows.

(1) *The bedload and suspended load transports are calculated as vertically-integrated instantaneous functions of near-bottom water velocity.* Field information leads us to believe that this assumption is valid for most natural beaches (Roelvink and Stive, 1989).
(2) *There is no threshold condition for initiation of sediment movement.* The implied assumption here is that most sediment transport occurs during very energetic conditions and a threshold is not required for the small amounts of sediment transport under low flow conditions. This is supported by the functional form of the stirring terms for bedload and suspended load, which are proportional to the third and fourth powers of velocity, respectively (Nairn and Southgate, 1993).
(3) *Lack of consideration of breaking-induced turbulence in the theoretical development of the stirring terms which are taken to be proportional to the bottom shear stress-induced turbulence alone.* However, the use of calibration data acquired from the surf zone ensures that this limitation will be compensated by the empirical efficiency factors (Nairn and Southgate, 1993).

Nairn and Southgate (1993) examined the possible values of the 'free or adjustable variables' in the Bailard (1981) model (i.e. the bed and suspended load efficiencies, and drag coefficient). In their study, Nairn and Southgate reviewed the existing values for bedload and suspended load efficiencies: Bagnold (1966) derived an expression for sediment transport (including bedload and suspended load components) in rivers, and suggested values for the bedload efficiency, ε_B, to be in the order of 0·13, and the suspended load efficiency, ε_S, to be 0·01. A later study by Bailard (1982) used a non-linear least-squares estimation procedure to obtain optimum bedload and suspended load efficiencies from the field measurements of the Nearshore Sediment Transport Study (NSTS) at Torrey Pines Beach, California (Seymour, 1989); the minimum mean-square error occurred for ε_B and ε_S values of 0·10 and 0·02, respectively. In agreement with the model applied by Nairn and Southgate (1993), these latter values for ε_B and ε_S have also been adopted here.

The drag coefficient, C_f, was derived, in this study, using a program (supplied by Hydraulics Research Ltd) based on a method presented by Soulsby (1997). Drag coefficient values were calculated for each 17·07 minute data run on each day, giving C_f values of between 0·005–0·011 (18 April 1991) and 0·006–0·015 (23 April 1991). Bed roughness, z_o, was derived using either $(2{\cdot}5/30)\,D_{50}$ for a flat bed (Engelund and Hansen, 1972), or $(25/30)\,\eta^2/\lambda$ for a rippled bed (Grant and Madsen, 1982), where η and λ are the ripple height and wavelength, respectively, and D_{50} is the median grain diameter. In the present work, the flat bed $z_o = 0{\cdot}000029\,\mathrm{m}$ and the rippled bed $z_o = 0{\cdot}0025\,\mathrm{m}$, based on an estimated ripple height of 0·03 m and ripple wavelength of 0·3 m (e.g. Dyer, 1986). From evidence presented by Davidson *et al*. (1993b) using the same dataset from Spurn Head, it was assumed that the sea bed inside and outside the surf zone was rippled. This rippled bed assumption also gave the best agreement with the observed fluxes.

The energetics approach assumption that the transports are calculated as vertically instantaneous functions of the near-bottom velocity means that it is usually taken that application is restricted to situations where the sea bed is flat (Bowen, 1980; Bailard, 1981). However, Nairn and Southgate (1993) refute this and state that during conditions when the majority of cross-shore sediment transport occurs, the advecting mechanisms of mean flow and wave skewness are so strongly directed shoreward or seaward, that the influence of ripples on a fluctuating

Table I. Largest terms in the cross-shore transport equation (Guza and Thornton, 1985). Positive values indicate onshore transport

Type	Term	Value	Factor	$V\times F$
Bedload	$\dfrac{\langle \lvert u \rvert^2 u\rangle}{U_m^3}$	0·06	$\varepsilon_B/\tan\phi$	0·02
	Others	⟨0·02		
Suspended load	$\dfrac{\langle \lvert u \rvert^3 u\rangle}{U_m^4}$	0·24	$\varepsilon_S\times U_m/W$	0·14
	Others	⟨0·04		

Table II. Largest terms (time-averaged values) in the cross-shore transport equation at Spurn Head, 18 April 1991

Type	Term	Value	Factor	$V\times F$
Bedload	$\dfrac{\langle \lvert u \rvert^2 u\rangle}{U_m^3}$	0·24	$\varepsilon_B/\tan\phi$	0·04
	Others	⟨0·02		
Suspended load	$\dfrac{\langle \lvert u \rvert^3 u\rangle}{U_m^4}$	0·56	$\varepsilon_S\times U_m/W$	0·11
	Others	⟨0·01		

Table III. Largest terms (time-averaged values) in the cross-shore transport equation at Spurn Head, 23 April, 1991.

Type	Term	Value	Factor	$V\times F$
Bedload	$\dfrac{\langle \lvert u \rvert^2 u\rangle}{U_m^3}$	0·07	$\varepsilon_B/\tan\phi$	0·015
	Others	⟨0·02		
Suspended load	$\dfrac{\langle \lvert u \rvert^3 u\rangle}{U_m^4}$	0·25	$\varepsilon_S\times U_m/W$	0·04
	Others	⟨0·01		

level of sediment concentration is inconsequential. Therefore, application of the energetics model seems to be appropriate in nearshore field situations where detailed changes in the bed roughness are not known.

Guza and Thornton (1985) looked at the relative magnitudes of the different components in Bailard's (1981) cross-shore transport model using measurements from the NSTS at Torrey Pines (Table I). The cross-shore velocity moments, $\langle \lvert u \rvert^2 u\rangle/U_m{}^3$ and $\langle \lvert u \rvert^3 u\rangle/U_m{}^4$, can be seen to have the greatest magnitude in the bedload and suspended load, respectively. Using the constant values (i.e. bedload and suspended load efficiencies, beach slope, angle of repose and sediment fall velocity) specified earlier (see Equation 1), the relative magnitudes of these terms can be evaluated for the Spurn Head measurements. Tables II and III show the dominant terms in the cross-shore transport equation for 18 and 23 April 1991, respectively.

Comparison of the Spurn Head moment measurements with those obtained by Guza and Thornton (Table I), shows remarkable similarity. The two skewness-type terms, $\langle \lvert u \rvert^2 u\rangle/U_m{}^3$ and $\langle \lvert u \rvert^3 u\rangle/U_m{}^4$, are clearly dominant in the bedload and suspended load parts of the transport equation. Although both these skewness terms contribute an onshore sediment flux, the suspended load term, $\langle \lvert u \rvert^3 u\rangle/U_m{}^4$, has the greater magnitude. Here, it is the suspended load term, $\langle \lvert u \rvert^3 u\rangle/U_m{}^4$, which will be examined more closely.

Following the work of Roelvink and Stive (1989) and assuming $\tilde{u} \rangle \bar{u}$ and u_S (short wave component) $\rangle\rangle$ u_L (long wave component), the suspended load parameter ($\langle | u |^3 u \rangle / U_m^4$), can be sub-divided into three component velocity terms (e.g. Foote and Huntley, 1994; Foote *et al*., 1994):

$$\begin{aligned} &\text{short waves} && \langle (u_S^2)^{3/2} u_S \rangle / U_m^4 \\ &\text{long waves} && \langle 4(u_S^2)^{3/2} u_L \rangle / U_m^4 \\ &\text{and mean flow} && \langle 4(u_S^2)^{3/2} \bar{u} \rangle / U_m^4 \end{aligned} \tag{5}$$

This enables a closer examination of the relative importance of the mean flow, long wave (wave periods greater than 20 s) and short wave (wave periods less than 20 s) components of flow, as shown in Foote (1994). In order to compare the suspended sand transport predictors with the measured suspended sand flux, the measured velocity moment was incorporated into the following simplified form of Equation 1 for the predicted cross-shore suspended sand transport rate, $\langle i_x \rangle_s$:

$$\langle i_x \rangle_S = \frac{\rho C_f \varepsilon_S}{W} U_m^4 \frac{\langle |u|^3 u \rangle}{U_m^4} \tag{6}$$

where each of the parameters assumes the definitions provided earlier. Equation 6 is a very simplified form of the original Bailard formula (Equation 1); considering only the suspended load, and using only the skewness term, $\langle | u |^3 u \rangle / U_m^4$, but based on Tables II and III, Equation 6 should be within approximately 30 per cent of the full prediction.

Integrated flux measurements

Concurrent optical backscatter sensor and cross-shore current velocity measurements provide some insight into the response of the near-bed suspended sand concentration (SSC) to the wave-induced flow (e.g. Hanes and Huntley, 1986; Doering and Bowen, 1988). Jaffe *et al*. (1984) measured cross-shore current velocity and SSCs across the surf zone during a storm and investigated the cross-shore suspended sediment fluxes using:

$$\begin{aligned} \overline{cu} &= \bar{c}\,\bar{u} + \overline{\tilde{c}\tilde{u}} \\ \text{Total} &= \text{Mean} + \underset{\substack{\downarrow \\ \text{Short wave}}}{\text{Oscillatory}} \quad \underset{\substack{\downarrow \\ \text{Long wave}}}{} \end{aligned} \tag{7}$$

Equation 7 represents the total cross-shore sediment transport rate, comprising both mean and oscillatory components, at any given height above the sea bed. In this expression, the first term represents the local sediment transport rate due to time-averaged quantities, $\bar{c}\,\bar{u}$, and the second term, the *flux coupling*, $\overline{\tilde{c}\tilde{u}}$, describes the net, time-averaged cross-shore transport induced by these oscillatory components. The total cross-shore sediment transport rate (Equation 7), can therefore be decomposed in a similar manner to the moment predictors of suspended sand transport, to yield mean flow, short wave and long wave contributions to the suspended sand transport.

A fundamental limitation of this approach is the existence of only point measurements of the current velocity and suspended sand concentration, when the velocity moment predictors of Bailard's expression refer to total, depth-integrated transport rates. In this study, a comparison of the moment predictions with the point suspended sand observations was achieved by assuming an exponential sediment concentration profile (e.g. Nielsen, 1979):

$$c(z) = c_o \, exp\,(-z/L_s) \tag{8}$$

The exponential relationship between sediment concentration and elevation above the bed has been advocated in many studies of sediment transport (e.g. Nielsen *et al*., 1982; Sternberg *et al*., 1984; Nielsen, 1988), where the

sediment suspension is supported by a simple diffusive mechanism. In Equation 8, c_o denotes the near-bed reference concentration (taken at the top of the bedload layer in sheet flow, or at the ripple crest for a rippled bed), L_s the vertical length scale of the decay and z the elevation above the sea bed. In the present study, the vertical length scale, L_s, for a rippled bed is defined, following Nielsen (1988), as:

$$L_S = \eta\{1{\cdot}24 \exp[-40(W/U_m)^2] + 0{\cdot}20\} \tag{9}$$

where η is the ripple height, W is the sediment settling velocity and U_m is the maximum orbital velocity, as defined in Equation 2. Assuming the wave velocity to be independent of depth, the flux profile will be the product of a constant and the concentration profile. Integrating the flux profile is then equivalent to integrating the concentration profile. If the height of the suspension measurement (i.e. the optical backscatter sensor level) is z_r:

$$c(z_r) = c_o \exp(-z_r/L_s) \tag{10}$$

Eliminating c_o from Equations 8 and 10:

$$c(z) = \frac{c(z_r)\exp(-z/L_S)}{\exp(-z_r/L_S)} \tag{11}$$

Integrating over z:

$$= \frac{c(z_r)}{\exp(-z_r/L_S)} \int_0^\infty \exp(-z/L_S)\,dz \tag{12}$$

$$= \frac{c(z_r)L_S}{\exp(-z_r/L_S)} \tag{13}$$

$$\therefore \text{Depth} - \text{integrated flux} = \text{Flux at sensor level} \times \frac{L_S}{\exp(-z_r/L_S)} \tag{14}$$

$$= \text{Flux measurement} \times \text{MF} \tag{15}$$

The expression enclosed in brackets in Equation 14 is used as a multiplying factor (MF). An estimate of the measured depth-integrated suspended sand flux is generated using the actual flux measurements at the reference level ($z_r = 0{\cdot}065$ m and $0{\cdot}10$ m for 18 and 23 April 1991, respectively) and the multiplying factor (MF). In order to give the depth-integrated flux in units of $\mathrm{N\,m^{-1}\,s^{-1}}$ (the same unit as the Bailard predictor) it was also necessary to multiply the above flux by g, the gravitational acceleration ($9{\cdot}81\,\mathrm{m\,s^{-2}}$):

$$= \text{Flux measurement} \times \text{MF} \times g \tag{16}$$

Fluxes calculated using this depth-integrated flux **measurement** equation (Equation 16) are now compared with fluxes calculated using the measurement-based velocity moment **predictor** expression (Equation 6).

RESULTS

The suspended load transport predictors and the depth-integrated flux profiles are highly dependent upon the choice of the drag coefficient C_f and the vertical length scale L_s values. In particular, choice of these values in Equations 6 and 14, determines whether there are flat bed/sheet flow or rippled bed conditions through the course of each tidal cycle. For the Spurn Head measurements examined in this work (18 and 23 April, 1991), the most appropriate drag coefficient and vertical length scale values were those relating to rippled bed conditions. The closest agreement between predictions and observations was obtained by assuming the sea bed to be rippled both shoreward and seaward of the breakpoint. On the basis of this assumption, the moment-based

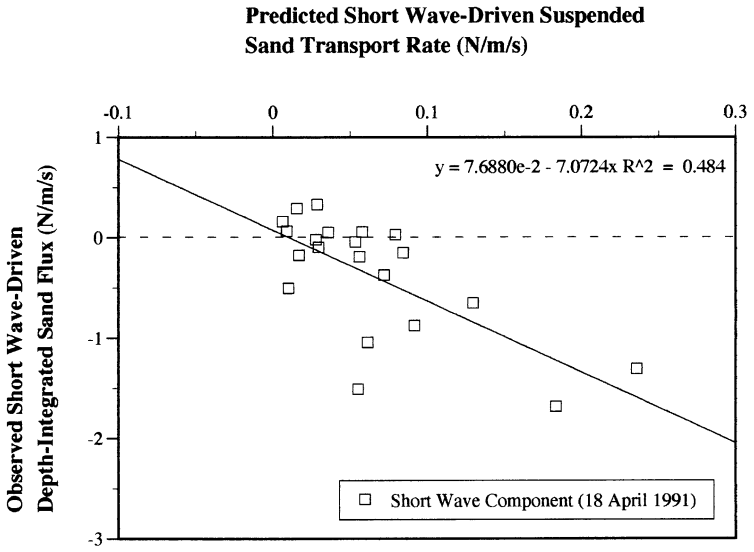

Figure 3. Predicted vs. Observed Short Wave-Driven Suspended Sand Transport (Rippled Bed) for 18 April, 1991.

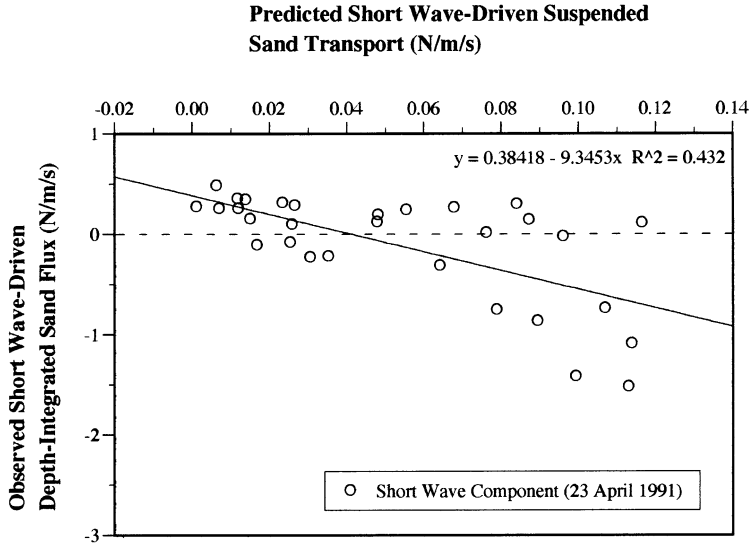

Figure 4. Predicted vs. Observed Short Wave-Driven Suspended Sand Transport (Rippled Bed) for 23 April, 1991.

predictions and depth-integrated flux observations were calculated for the Spurn Head data. Predicted and observed measurements were evaluated for the short wave, long wave and mean flow modes of suspended sand transport and also the net suspended load transport. Comparison of each component of transport provides some indication of the degree of correlation between model and field results.

Short wave component, $\overline{(u_s^2)^{3/2}u_s}$

The short wave velocity term represents short wave skewness (a sediment stirring parameter) coupled with short wave velocity which, in turn, mobilizes and transports the suspended sediment; the corresponding depth-integrated flux term couples the short period motion and its equivalent sediment response. Figures 3 and 4 show the comparison between the predicted and observed short wave-driven suspended load transport for the two days, 18 and 23 April 1991, respectively. This comparison reveals the degree of correlation between the moment-based predictions and the depth-integrated suspended sand flux measurements. The most noticeable

feature, in both Figures 3 and 4, is the negative correlation which arises between these predictions and observations, with low regression values in both cases ($R^2 = 0{\cdot}484$ for 18 April; $R^2 = 0{\cdot}432$ for 23 April). In addition, the regression line on Figures 3 and 4 does not pass through the origin (0, 0), as would have been expected.

It is evident that the predictions do not agree well with the observations. In particular, where onshore transport is predicted, the measurements often show the opposite case to be true with predominantly offshore transport. Such a result would be expected over a rippled bed where suspended sand transport at incident wave frequencies occurs in the direction opposite to that of the strongest flow. This results from the skewness of the incoming waves, whereby the strong onshore flow under the wave crest generates sediment-laden vortices in the lee of the ripples, which are subsequently ejected at times of flow reversal and the sediment is transported offshore by the weaker offshore flow.

If the *sign* of transport is ignored, the *magnitude* is under-predicted. In Figures 3 and 4, it is evident that the magnitude of the incident wave-driven transport was under-predicted by a factor of ≈6 for 18 April, and a factor of ≈7 for 23 April.

Long wave component, $\overline{4(u_S^2)^{3/2}u_L}$

This long wave velocity term combines short wave skewness (mobilising the sediment) with long wave velocity (transporting the sediment) and, as before, the accompanying depth-integrated flux term couples long period motion with the long wave frequency sediment suspension. In Figures 5 and 6, the predicted and observed long wave-driven suspended load transport values are compared for 18 and 23 April, respectively. The relationship between model prediction and field measurement of long wave-driven transport is a considerable improvement on the short wave analysis. Predicted long wave and measured transport results are positively correlated, and the regression line passes close to the origin. Regression coefficients are much higher between these long wave-related transport predictions and observations, with $R^2 = 0{\cdot}782$ and $0{\cdot}548$ for the days 18 and 23 April, respectively. Overall, transport due to long period motion was under-predicted by factors of approximately 7 and 8 (18 and 23 April, respectively). As with the short wave component, the model is generally under-predicting the transport magnitude by a factor of about 7.

Mean flow component, $\overline{4(u_s^2)^{3/2}\bar{u}}$

Comparison between the mean flow moment-based predictor and the measured mean flow-driven depth-integrated suspended sand flux is shown in Figures 7 and 8 for the two days, 18 and 23 April, respectively. Predicted mean flow and measured transport values, like the long wave results, are positively correlated with the regression line passing close to the origin, and even higher regression coefficients ($R^2 = 0{\cdot}887$ for 18 April and $R^2 = 0{\cdot}870$ for 23 April, 1991). It appears, therefore, that for the mean flow component the moment-based predictor is good. The fact that the model is under-predicting by a factor of between 10 and 15 is probably because no boundary layer was used to reduce the near-bed velocities in the calculation of the 'observed' depth-integrated fluxes.

Total suspended load transport rate, $\langle i_x \rangle_s$

Total cross-shore suspended sand transport predictions/observations are shown for both 18 and 23 April, in Figures 9 and 10. There is a large degree of scatter in both diagrams and generally very little agreement between the estimated total transport rates and the corresponding measured values. This lack of agreement is not wholly unexpected, owing to the problems encountered earlier in predicting the direction (sign) of short wave transport.

Since the direction of the short wave transport was predicted incorrectly, we have adapted the Bailard model by summing the mean flow and long wave components, and *subtracting* the short wave component, in order to compensate for the 'reverse' sediment transport and, in turn, the negative sign of the short wave parameter. The resultant values for this adapted predictor of total suspended sediment transport rate are compared with observed total suspended sand flux (Figures 11 and 12). The results show that this adapted predictor yields a reasonable estimate of total transport (which is under-predicted by a factor of about 8 or 9). However, there is a worrying offset: for zero observed net suspended sand flux, the adapted predictor of total suspended sediment

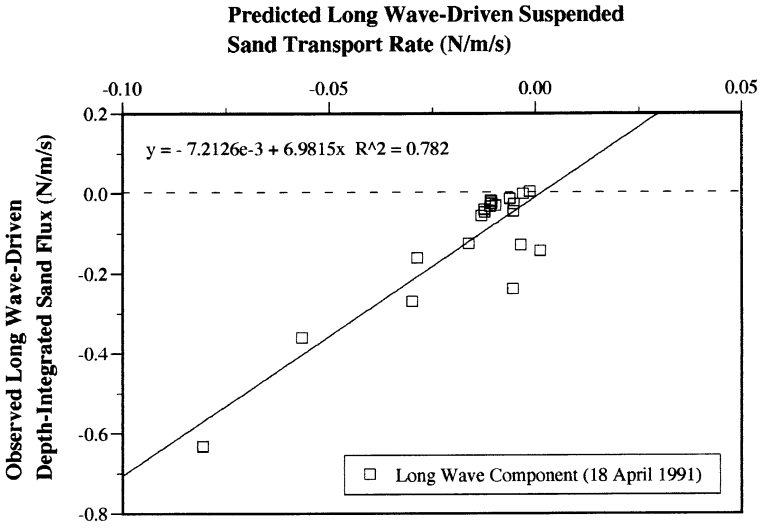

Figure 5. Predicted vs. Observed Long Wave-Driven Suspended Sand Transport (Rippled Bed) for 18 April, 1991.

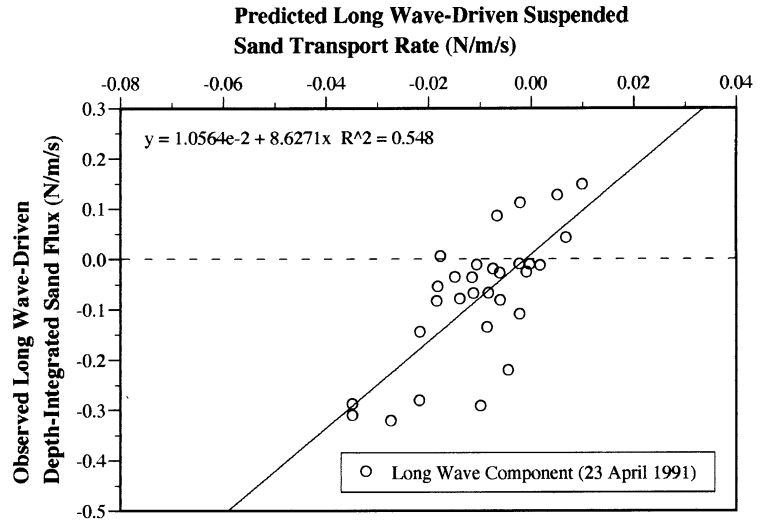

Figure 6. Predicted vs. Observed Long Wave-Driven Suspended Sand Transport (Rippled Bed) for 23 April, 1991.

transport rate gives a negative value (offshore) of 0·02 to 0·05 $N m^{-1} s^{-1}$ (for the two days). Clearly, further problems in the predictive scheme exist which are yet to be resolved.

DISCUSSION

This study extends earlier assessment of energetics-based approaches to modelling cross-shore sand transport (e.g. Guza and Thornton, 1985; Bailard, 1987; Foote and Huntley, 1994; Foote *et al.*, 1994; Kroon, 1994). Such energetics models of cross-shore sand transport offer a simple, plausible method for estimating the movement of sediment across a beach profile under a range of wave and current conditions. Direct comparison with Bailard's (1987) theoretical predictions has shown close agreement in the behaviour of some surf zone cross-shore transport equation velocity moments, but poor agreement in others.

In our previous studies, despite examination of field measurements with a range of characteristics, velocity moment values have shown broadly similar cross-shore patterns. This gives some encouragement in using such moments to provide simple models of macrotidal beach profile evolution (e.g. Foote *et al.*, 1994). However, the

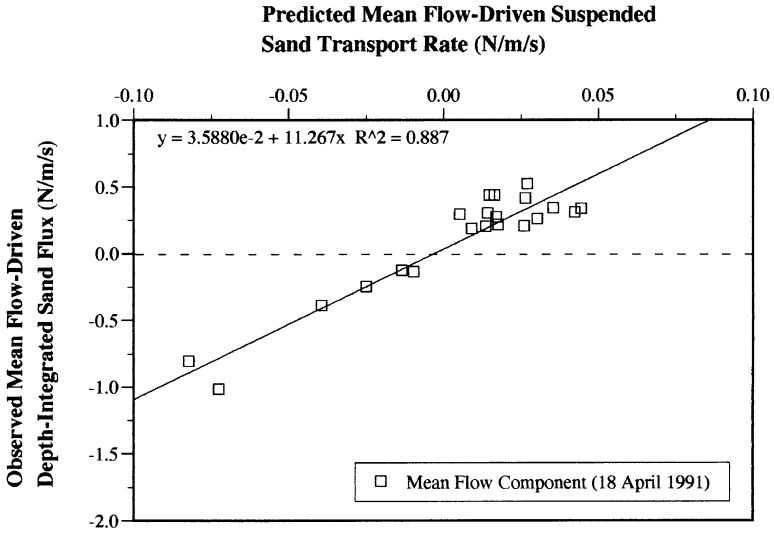

Figure 7. Predicted vs. Observed Mean Flow-Driven Suspended Sand Transport (Rippled Bed) for 18 April, 1991.

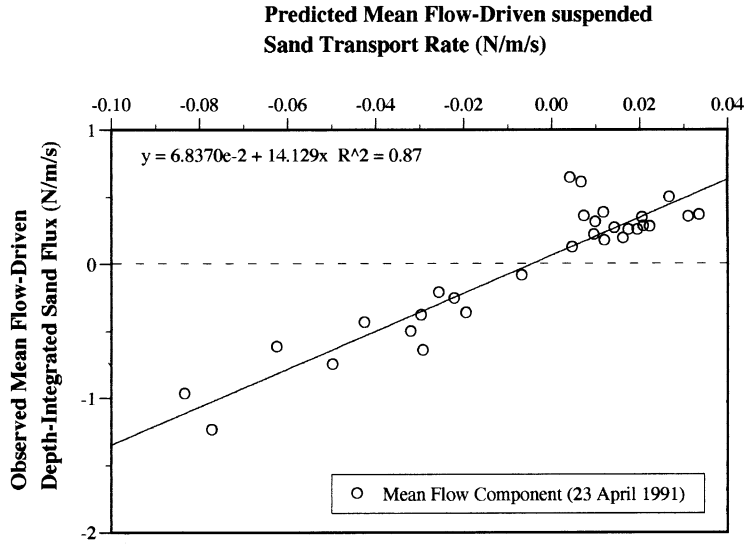

Figure 8. Predicted vs. Observed Mean Flow-Driven Suspended Sand Transport (Rippled Bed) for 23 April, 1991.

primary question that has to be addressed is whether these moment-based energetics predictions are sufficiently accurate to give reliable quantitative predictions of surf zone sediment transport rates. In order to put these results into context, the significance of some of the assumptions that have been made in this contribution is now considered.

To make a suitable comparison between the depth-integrated transport equation and point measurements of sand fluxes required a multiplying factor to summarize depth-integration. Based upon the most simple assumption of an exponential concentration profile and a wave velocity independent of depth, the suspended sand flux profile was taken to be the product of the multiplying factor and the measured suspended sand flux at a single known height above the bed. In doing this, it was assumed that the flux profile for all three components (mean, long and short) takes the form of the wave-averaged concentration profile, with a length scale L_s based primarily on the ripple height according to Equation 12. For mean flows, use of the wave-averaged $c(z)$ is reasonable, but should be multiplied by a boundary layer profile of velocity which would improve the value of MF, and hence improve the fit of the data. For the oscillatory flows, in essence we are assuming that at every

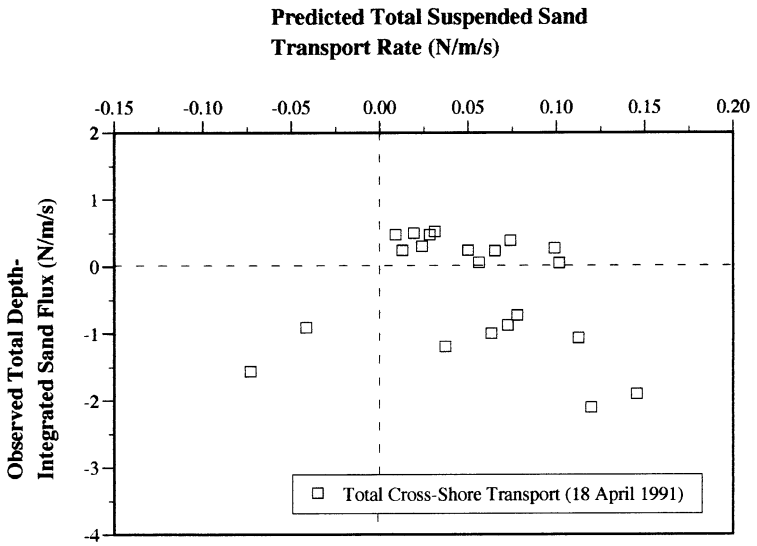

Figure 9. Predicted vs. Observed Total Cross-Shore Suspended Sand Transport (Rippled Bed) for 18 April 1991

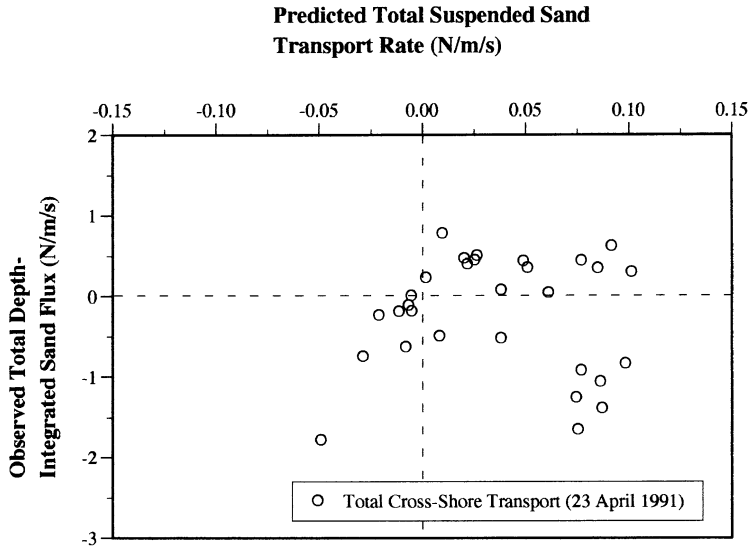

Figure 10. Predicted vs. Observed Total Cross-Shore Suspended Sand Transport (Rippled Bed) for 23 April 1991

instant through the wave cycle the flux profile takes the exponential $c(z)$ form, with L_s independent of the instantaneous magnitude of the flow. Although this seems a poor analogue of what happens, a more satisfactory alternative would require detailed modelling beyond the scope of this initial study.

Naturally, the use of time- and depth-averaged flow and suspended load parameters does not allow a consideration of the vertical variations which occur in the cross-shore flows and suspended sediment flux. This is a known disadvantage of the Bailard transport model which disregards the existence of possible phase differences between flow and sediment response. Furthermore, the field data include points from both inside and outside the surf zone which are physically very different environments. Despite these complications, through a first order comparison of the moment-based suspended load transport predictions with depth-integrated suspended sand flux measurements, a reasonable degree of correlation between model and field results has been obtained.

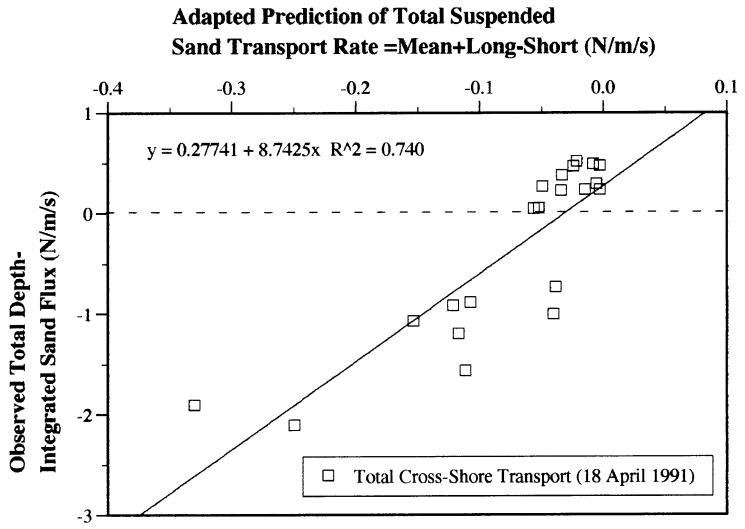

Figure 11. Adapted Predictions vs. Observed Total Cross-Shore Suspended Sand Transport (Rippled Bed) for 18 April, 1991.

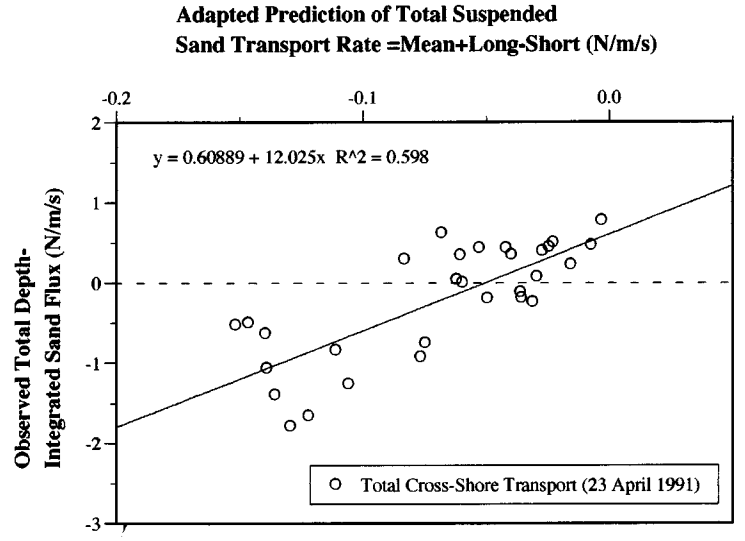

Figure 12. Adapted Predictions vs. Observed Total Cross-Shore Suspended Sand Transport (Rippled Bed) for 23 April, 1991.

CONCLUSIONS

By comparing simple energetics predictions, based on measured velocity moments, with depth-integrated suspended sand fluxes based on point measurements, we can draw the following conclusions.

(1) *Short waves*: the transport *magnitude* is under-predicted by less than an order of magnitude. However, the transport *direction* is incorrectly predicted. The model predicts onshore transport, while the measurements show offshore transport, as would be expected for 'reverse' transport over ripples.
(2) *Long waves*: the transport is under-predicted by less than an order of magnitude, and is in the correct direction, which is predominantly offshore.
(3) *Mean Flow*: the transport is under-predicted by just over an order of magnitude, and is in the correct direction, which is also predominantly offshore. The model/data comparison gave the highest regression

values for this component of the transport. The magnitude predictions could be improved by adding a boundary layer profile to the measured velocities.

This study has shown the potential for velocity moment-based predictions of cross-shore sand transport on beaches. Despite the simple assumptions made, suspended sand transport magnitudes associated with short wave, long wave and mean flow motions, were all predicted to about an order of magnitude. To improve these types of predictions further, more detail is needed on the vertical profiles of velocity and suspension, and changes in bed roughness.

ACKNOWLEDGEMENTS

This work was carried out with the support of a grant from the Natural Environment Research Council (NERC Grant No. GR9/1484): Sand Transport on Macrotidal Beaches.

REFERENCES

Bagnold, R. A., 1956. 'The flow of cohesionless grains in fluids', *Philosophical Transactions of the Royal Society, London, Series A*, **249**, 964, 235–297.

Bagnold, R. A. 1963. 'Mechanics of marine sedimentation', in *The Sea: Ideas and Observations*, Volume 3, Interscience Publishers, New York, 507–528.

Bagnold, R. A. 1966. *An approach to the sediment transport problem from general physics*, US Geological Survey Professional Paper **422-I**, 37 pp.

Bailard, J. A. 1981. 'An energetics total load sediment transport model for a plane sloping beach', *Journal of Geophysical Research*, **86**(C11), 10 938–10 954.

Bailard, J. A. 1982. 'Modeling on-offshore sediment transport in the surfzone', *Proceedings of the 18th International Conference on Coastal Engineering*, Cape Town, ASCE, 1419–1438.

Bailard, J. A. 1987. 'Surf zone wave velocity moments', *Proceedings of the Coastal Hydrodynamics Conference*, ASCE, 328–342.

Bailard, J. A. and Inman, D. L. 1981. 'An energetics bedload model for a plane sloping beach: local transport', *Journal of Geophysical Research*, **86**(C3), 2035–2043.

Bowen, A. J. 1980. 'Simple models of nearshore sedimentation; beach profiles and longshore bars', in: McCann, S. B. (Ed.), *The Coastline of Canada*, Geological Survey of Canada, Ottawa, Paper **80-10**, 1–11.

Davidson, M. A., Russell, P. E., Huntley, D. A., Hardisty, J. and Cramp, A. 1993a. 'An overview of the British Beach and Nearshore Dynamics (B-BAND) programme', *Proceedings of the 23rd International Conference on Coastal Engineering*, Venice, 1987–2000.

Davidson, M. A., Russell, P. E., Huntley, D. A. and Hardisty, J. 1993b. 'Tidal asymmetry in suspended sand transport on a macrotidal intermediate beach', *Marine Geology*, **110**, 333–353.

Doering, J. R. C. and Bowen, A. J. 1988. 'Wave-induced flow and nearshore suspended sediment', *Proceedings of the 21st International Conference on Coastal Engineering*, Malaga, ASCE, 1452–1463.

Dyer, K. 1986. *Coastal and Estuarine Sediment Dynamics*, John Wiley and Sons, Chichester, 342 pp.

Engelund, F. and Hansen, E. 1972. *A Monograph on Sediment Transport in Alluvial Streams*, Technical Press, Copenhagen, 62 pp.

Foote, Y. L. M. 1994. *Waves, Currents and Sand Transport Predictors on a Macro-Tidal Beach*, PhD thesis, University of Plymouth, 257 pp.

Foote, Y. L. M. and Huntley, D. A. 1994. 'Velocity moments on a macro-tidal intermediate beach', *Proceedings of the Coastal Dynamics '94 Conference*, Barcelona, 794–808.

Foote, Y. L. M., Huntley, D. A. and O'Hare, T. J. 1994. 'Sand transport on macrotidal beaches', *Proceedings of the Euromech 310 Colloquium*, Le Havre, 360–374.

Grant, W. D. and Madsen, O. S. 1982. 'Movable bed roughness in unsteady oscillatory flow', *Journal of Geophysical Research*, **87**(C1), 469–481.

Guza, R. T and Thornton, E. B. 1985. 'Velocity moments in nearshore', *Journal of Waterway, Port, Coastal and Ocean Engineering*, **111**(2), 235–256.

Hanes, D. M. and Huntley, D. A. 1986. 'Continuous measurements of suspended sand concentration in a wave dominated nearshore environment', *Continental Shelf Research*, **6**(4), 585–596.

Hoad, J. 1991. 'Monitoring of the response of the inter-tidal beach profile to tidal and wave forcing', *Proceedings of the Coastal Sediments '91 Conference*, Seattle, 385–395.

Jaffe, B., Sternberg, R. W. and Sallenger, A. H. 1984. 'The role of suspended sediment in shore-normal beach profile changes', *Proceedings of the 19th International Conference on Coastal Engineering*, Houston, ASCE, 1983–1996.

Kroon, A. 1994. *Sediment Transport and Morphodynamics of the Beach and Nearshore Zone near Egmond, The Netherlands*, PhD thesis, Utrecht, 275 pp.

Mason, S. J. and Hansom, J. B. 1988. 'Cliff erosion and its contribution to a sediment budget for part of the Holderness Coast, England', *Shore and Beach*, **56**(4), 30–38.

Nairn, R. B. and Southgate, H. N. 1993. 'Deterministic profile modelling of nearshore processes. Part 2. Sediment transport and beach profile development', *Coastal Engineering*, **19**, 57–96.

Nielsen, P. 1979. *Some Basic Concepts of Wave Sediment Transport*, Series Paper No. **20**, Institute of Hydrodynamics and Hydraulics Engineering, Technical University of Denmark, 160 pp.

Nielsen, P. 1988. 'Three simple models of wave sediment transport', *Coastal Engineering*, **12**, 43–62.
Nielsen, P., Green, M. O. and Coffey, F. C. 1982. *Suspended Sediment Under Waves*, Technical Report **82/6**, Coastal Studies Unit, University of Sydney.
Pringle, A. W. 1985. 'Holderness coast erosion and the significance of ords', *Earth Surface Processes and Landforms*, **10**, 107–124.
Roelvink, J. A. 1993. *Surf Beat and its Effect on Cross-shore Profiles*, Delft Hydraulics, 116 pp.
Roelvink, J. A. and Stive, M. J. F. 1989. 'Bar-generating cross-shore flow mechanisms on a beach', *Journal of Geophysical Research*, **94**(C4), 4785–4800.
Russell, P. E., Davidson, M. A., Huntley, D. A., Cramp, A., Hardisty, J. and Lloyd, G. 1991. 'The British Beach And Nearshore Dynamics (B-BAND) programme', *Proceedings of the Coastal Sediments '91 Conference*, Seattle, ASCE, 371–384.
Seymour, R. J. 1989. *Nearshore Sediment Transport*, Plenum Press, New York, 450 pp.
Short, A. D. 1991. 'Macro-meso tidal beach morphodynamics – An overview', *Journal of Coastal Research*, **7**(2), 417–436.
Soulsby, R. L. 1997. *Dynamics of Marine Sands*, Report No. **SR466**, Hydraulics Research Ltd, Wallingford, Oxon, UK.
Sternberg, R. W., Shi, N. C. and Downing, J. P. 1984. 'Field investigations of suspended sediment transport in the nearshore zone', *Proceedings of the 19th International Conference on Coastal Engineering*, Houston, 1782–1798.

